

SCIENTIFIC REPORTS



OPEN

Heterogeneous Catalytic Oxidation of Amides to Imides by Manganese Oxides

Sourav Biswas^{1,4}, Harshul S. Khanna², Quddus A. Nizami³, Donald R. Caldwell¹, Katherine T. Cavanaugh¹, Amy R. Howell¹, Sumathy Raman³, Steven L. Suib^{1,2} & Partha Nandi³

Herein, we report a one-step peroxide mediated heterogeneous catalytic oxidation of amides to imides utilizing a series of manganese oxides. Among them, Cs/Mn₂O₃ was found to be the most active catalyst for the selective partial oxidation of *N*-benzylbenzamide to diphenyl imide. We have been able to apply an optimized oxidation method to other aromatic substrates. The feasibility of using air as an oxidant, the heterogeneous nature, inexpensive catalytic materials, respectable turnover numbers, and chemoselectivity to imides make this methodology an attractive choice for functional group transformations of amides to imides.

Imide functional groups have versatile applications in pharmaceutical, polymer, and natural product synthesis^{1,2}. Traditionally imides have been synthesized by reaction between dicarboxylic acid e.g., phthalic acid (or anhydride) and amines³. Acylation of amides⁴, and rearrangement of isocyanates can also yield imides⁵. A few homogeneous catalytic oxidations of amides to imides are reported recently using organic hydroperoxides as terminal oxidants^{6–8}.

Manganese oxides have gained wide recognition as powerful materials in catalytic oxidation reactions^{9,10}. Readily accessible multiple oxidation states, high abundance, thermally stable structural forms, and dioxygen reduction ability are some of the important properties of these materials^{11–13}. Several promoter ions can reside as structural or charge balancing ions to enhance the catalytic activity of manganese oxides^{14–16}. Moreover, the diversity of synthetic methods allows preparation of different forms of manganese oxide of varying porosity and crystallinity such as octahedral molecular sieves (OMS), octahedral layer (OL), amorphous manganese oxide (AMO), birnessite, α -manganese oxide, and mesoporous manganese oxide¹¹. These mixed valent, high surface area materials have excellent redox properties which lead to highly efficient manganese based oxidation catalysts. The effect of ion promotion in the manganese oxides has been studied previously¹⁷. One proposed mechanism is that with cesium ion promotion in manganese oxides, the surface tends to induce a more basic character, which allows the binding energy for lattice oxygen to be lowered^{17,18}. Manganese oxide based materials have been utilized in different types of catalytic oxidation reactions such as selective oxidation of alcohols to aldehydes¹⁹, hydrocarbons to alcohols and ketones²⁰, styrenes to styrene oxides²¹, alcohols to amides^{22–26}, and amines to imines^{27–29}. Furthermore, manganese oxide catalysts are effective in oxidative coupling of alkynes³⁰, alkyne-silanes³¹, and alkyne-amine³². Herein, we report a heterogeneous catalytic oxidation of benzylic amides to imides by two different classes of manganese oxides.

Results and Discussion

***N*-benzylbenzamide Oxidation.** Initially we utilized the oxidation of *N*-benzylbenzamide as the model reaction for developing the optimal reaction conditions³³. In our early screening attempts, we used a number of redox active metal oxides (e.g., BiVO₄, CuMoO₄, CoMoO₄) without much success. In a few cases, over-oxidation of the imide and thermal cracking reactions were observed. This was, however, not the case with Mn oxides. Building on our recently employed mesoporous manganese oxide material as a highly active oxidation

¹Department of Chemistry, University of Connecticut, Storrs, CT, 06269, USA. ²Institute of Materials Science, University of Connecticut, Storrs, CT, 06269, USA. ³Corporate Strategic Research, ExxonMobil Research and Engineering Company, 1545 US 22 East, Annandale, NJ, 08801, USA. ⁴Present address: Department of Chemistry, University of Wisconsin-Madison, 1101 University Avenue, Madison, WI, 53706, USA. Correspondence and requests for materials should be addressed to S.L.S. (email: steven.suib@uconn.edu) or P.N. (email: partha.nandi@exxonmobil.com)

Entry	Oxidant	Additives	Conv. (%) ^b	Selectivity (%) ^b	
				Diphenyl Imide	N-benzamide
1	Air	none	0	nd	nd
2	Oxygen	none	0	nd	nd
3	H ₂ O ₂	none	0	nd	nd
4	TBHP/water	none	5	50	22
5	TBHP/nonane	none	10	15	80
6 ^c	TBHP/nonane	NHPI ^d	25	90	10
7 ^e	TBHP/nonane	NHPI	90 (85)	95	5
8	THBP/nonane	Air	10	15	80
9	TBHP/nonane	Argon	0	nd	nd
10 ^f	None	NHPI	5	80	10
11	None	NHPI	0	nd	nd
12 ^f	TBHP/nonane	NHPI	0	nd	nd

Table 1. Optimization of oxidation of *N*-benzylbenzamide. ^aReaction conditions: *N*-benzyl benzamide (100 mg, 0.5 mmol, 1.0 equiv), meso Cs/Mn₂O₃ (50 mg), acetonitrile (5 mL, 95 mmol, 190 equiv), 80 °C, TBHP (5 mmol, 0.45 g, 10 equiv), 22 h. ^bConversions and selectivities were determined by GC-MS based on concentration of *N*-benzyl benzamide using *m*-xylene as internal standard. Isolated yields are in parentheses. ^cTBHP addition rate of 0.8 μL min⁻¹. ^d10 mol% NHPI. ^eMolecular sieves as additives (200 mg) and air. ^fNo catalyst. nd = not detected by GC-MS.

catalyst^{17,34–36}, a minute amount (0.14%) of electropositive Cs ions has been introduced in the manganese oxide structure, which enhanced the oxidation ability of manganese oxide by several orders of magnitude (100 fold) in oxidations of alcohols to aldehydes and amines to imines^{17,35}. Herein, Cs⁺ promoted mesoporous manganese oxide (meso Cs/Mn₂O₃) was used as a model catalyst and acetonitrile as the model solvent. In early attempts, the use of air and oxygen as the oxidant did not produce any product (Entries 1 and 2, Table 1). Using H₂O₂ also did not give any product (Entry 3, Table 1). We then switched our attention to *tert*-butyl hydroperoxide (TBHP in water) as the oxidant. TBHP is a popular oxidant for oxidation of inert C-H bonds due to high thermal stability and solubility^{37,38} as compared to H₂O₂. The reaction was performed then with different loadings of catalyst and TBHP (Entries 1–4, Table S1). The reaction was then performed with solvents of different polarities at their respective boiling points (Entries 4–8, Table S1). No imide was detected using dioxane, THF, or toluene. Chloroform and CH₂Cl₂ were avoided due to potential generation of COCl₂. (Entry 8, Table S1). Consequently, acetonitrile (ACN) was chosen as solvent for further reactions. The formation of another product (benzamide) can be attributed to the hydrolysis of intermediates.

***tert*-Butylhydroperoxide (TBHP) Decomposition.** The rate of hydrolysis and subsequent formation of benzamide was increased with increasing concentration of the TBHP/water. To suppress the hydrolysis, TBHP in nonane (5.5 M, in molecular sieves) was used as the oxidant, minimizing the amount of water. Using TBHP in nonane, a maximum conversion of 10% and lower selectivity (15%) to imide (Entry 5, Table 1) was obtained. Negligible amounts of nonanol and nonanone were observed due to oxidation of nonane. To evaluate the rate of decomposition of TBHP, we probed the rate of decomposition of TBHP in the absence of amide substrate. Almost all of the TBHP was consumed within 45 min of reaction (Table S2). Alternatively, conjugated organic nitroxyl radicals combined with transition metal co-catalysts have been shown to be powerful catalytic systems for the auto-oxidation of hydrocarbons. Among those, *N*-hydroxyphthalimide (NHPI) is very popular in metal catalyzed oxidation of hydrocarbons³⁹. Peroxyl radicals (ROO·) initiated by thermal decomposition of peroxides such as TBHP or deliberate introduction of free radical initiators, abstract an H-atom (>NO-H) from NHPI to form the PINO· radical (phthalimide *N*-oxyl)⁴⁰. The combination of TBHP in nonane being added slowly (0.8 microliter/min) and using NHPI as an oxidation promoter (10 mol%) proved to be successful, as a significant increase in conversion (25%) was observed with high selectivity (90%) for imide (Entry 6, Table 1) was observed. Using molecular sieves as water scavengers, we surmised that adventitious water could be scavenged which would otherwise cause undesirable hydrolysis of imides. Thus the best conversion (90%) and selectivity (95%) towards imide were obtained (Entry 7, Table 1) with NHPI and molecular sieves.

Using air as oxidant decreased amide conversion (10%) significantly (Entry 8, Table 1) but showed the feasibility of using air as an oxidant. TBHP and NHPI without any catalyst did not produce any imide (Entry 12, Table 1); this signified the role of manganese oxide as catalyst in this reaction. Upon repeating the reaction under an argon atmosphere, we did not detect any imide, which proved the role of O₂ as oxidant (Entry 9, Table 1). These results demonstrate the effectiveness of manganese oxides as heterogeneous catalysts for oxidation of amides to imides. The isolated yield (Entry 7) is in good agreement with the yield from GC-MS methods.

The oxidation of *N*-benzylbenzamide using Cs/Mn₂O₃ was then compared to different active, well known manganese oxide catalysts. Meso Mn₂O₃ having no Cs promoter ions showed much lower selectivity towards imide (Entries 1–2, Table 2). Cation vacancies in these oxides are the binding sites for amides based on our prior work where³⁵ small loading (0.16% by weight) of Cs in the meso Cs/Mn₂O₃ material was critical for oxidation of amines to imines (which was used in this study). Using potassium containing manganese oxide octahedral molecular sieves (prepared by solvent free methods, K-OMS-2-SF) having similar Cs loading (0.16%), conversion and

Entry	Catalyst	Conv. (%) ^b	Selectivity (%) ^b	
			Diphenyl Imide	N-benzamide
1 ^c	K-OMS-2	45	60	40
2 ^c	Meso Mn ₂ O ₃	50	60	40
3	Meso Cs/Mn ₂ O ₃	77	67	33
4	Cs-K-OMS-2 (SF)	60	15	85
5	AMO (UCT-1)	60	60	40
6	C-MnO ₂	15	50	50
7	None	0	nd	nd

Table 2. Catalyst Scope for oxidation of *N*-benzylbenzamide. ^aReaction conditions: *N*-benzylbenzamide (100 mg, 0.5 mmol, 1.0 equiv), catalyst (50 mg), acetonitrile (5 mL, 95 mmol, 190 equiv), TBHP (5 mmol, 0.45 g, 10 equiv) with addition rate of 0.8 $\mu\text{L min}^{-1}$, NHPI (8 mg, 0.05 mmol, 0.1 equiv), molecular sieves (200 mg), 80 °C, 22 h. ^bConversions and selectivities were determined by GC-MS based on concentration of *N*-benzylbenzamide using *m*-xylene as internal standard. ^cNo NHPI was used. C-MnO₂ denotes commercial manganese oxide. nd = not detected by GC-MS.

selectivity for imide decreased (Entry 4, Table 2). On the other hand, amorphous manganese oxide (AMO) prepared by redox methods displayed high conversion and selectivity (Entry 5, Table 2) to imides. Commercial manganese oxide was able to achieve minimal conversion without preferential selectivity towards the imide (Entry 6, Table 2). The reaction revealed no conversion in the absence of a catalyst (Entry 7, Table 2).

Substrate Scope. The substrate scope and limitations were then explored for different types of amides. This methodology works well for oxidation of activated (e.g. benzylic CH₂) α -CH₂ groups with respect to amide. AMO was able to oxidize aromatic (Entries 1, 2, 4–7, Table 3), lactam (Entry 6, Table 3), and heteroaromatic (Entry 7, Table 3) amides to corresponding imides with excellent conversion and selectivity. No side reaction was detected in the case of a benzamide with a *para*-chloro substitution (Entry 2, Table 3). However, to our surprise with *ortho*-chloro substitution in the benzamide, no imide formation was detected (Entry 3, Table 3). Oxidation of 1-isoinoline (Entry 6, Table 3) was facile and produced a cyclic imide with excellent conversion (>99%) and selectivity (100%). The yields from GC-MS studies are in reasonable agreement with isolated yields. A thiophene amide was converted to the imide effectively (Entry 7, Table 3) without oxidizing the sulfur to sulfoxide or sulfone. We used α methyl-substituted *ortho* carboxylic derivative of benzyl amide to investigate if a product related to the initial stage of oxidation could be isolated (complete oxidation to the imide would be impossible). However, the substrate was totally inert (Entry 8, Table 3), which may be due to difficult abstraction of N-H hydrogen atoms due to a steric effect of the methyl group. Unactivated aliphatic amides (Entries 9 and 10, Table 3) were not converted to imides using this procedure. This may be rationalized by the strength of α -CH bonds in those substrates that falls outside the range of the NHPI derived PINO radical's C-H activation scope.

Kinetic and Stability Studies. Time dependent experiments for the oxidation of *N*-benzyl benzamide were conducted using meso Cs/Mn₂O₃ to study reaction rates (Fig. S1a). Periodic sampling was undertaken, the catalyst was separated by filtration, and conversion and selectivity of the filtrate were determined by GC-MS. Two separate time dependent experiments with and without NHPI were conducted. In the absence of NHPI, the reaction was very sluggish at the beginning (5% conversion after 8 h), whereas the presence of NHPI accelerated the reaction. Experiments with TBHP and NHPI indicated a first order rate equation with respect to amide (Fig. S1b) having a rate constant of 0.0025 min⁻¹. PINO radical can abstract a hydrogen atom from amide (RCOCH₂NH₂) to initiate the reaction (Fig. S5). Since the addition rate of TBHP is slow, at the beginning the amount of TBHP was not enough for the generation of PINO radical. PINO radical reacts much faster than other peroxide based radicals with hydrocarbons, as confirmed by relative rate constants⁶. The catalyst stability was verified by performing reusability studies (Fig. S2b) with meso Cs/Mn₂O₃. After reaction, the catalyst was filtered, washed with excess solvent and water, dried under vacuum and reactivated at 250 °C for 30 min. No apparent loss of activity was observed after 3 catalytic cycles. Moreover, from the powder X-ray diffraction studies (Fig. S2a), it is apparent that the amorphous nature of the catalyst is retained after multiple reuses.

Possible Reaction Pathway. We investigated the relative rates of oxidation of *para* substituted *N*-benzylbenzamides (*p*-Cl, *p*-H, *p*-Me, *p*-OMe) to determine the electronic effect of the substituents. The Hammett equation can be used to interpret the electronic or steric influence of the substituents on the reaction intermediates. A linear relationship was found between $\ln(k_X/k_H)$ and the Brown–Okamoto constant (σ_p^+) (Fig. 1). The slope of the plot resulted in a reaction constant (ρ) value of 0.355, which signified involvement of a partial negative charge at the reaction center in the transition state of the rate-limiting step (polar effects in similar radical reactions are known)⁶.

We propose a series of steps that can contribute to the formation of imides by manganese oxide (Fig. S3). Adsorbed amide molecules transfer an electron to the Mn center, followed by a cleavage of α C-H bond mediated by the NHPI/MnO_x system (Fig. S3). The oxidation of an alpha substituted amide is almost undetectable under the present reaction conditions, where the presence of the methyl group could have hindered the binding of amide, thus blocking the cleavage of the α C-H bond. The reaction pathway in theory may involve an imine intermediate, by further removal of proton and electron transfer to Mn atoms (Fig. 2). However according to the

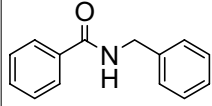
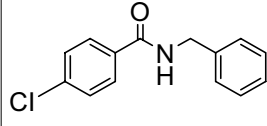
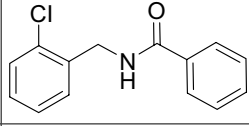
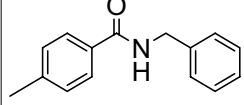
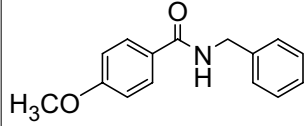
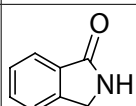
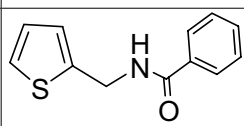
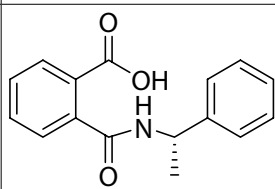
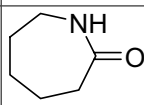
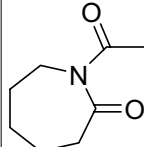
Entry	Substrate	Conv. (%) ^b	Selectivity (%) ^b (Imide)
1 ^c		90 (85)	95
2		90 (79)	98
3		0	0
4		92	94
5		90	94
6 ^c		>99 (61)	100
7		85	92
8		0	0
9		0	0
10		0	0

Table 3. Oxidation of amides to imides by manganese oxides. ^aReaction conditions: Amide (0.5 mmol, 1.0 equiv), AMO (50 mg), acetonitrile (5 mL, 95 mmol, 190 equiv), TBHP (5 mmol, 0.45 g, 10 equiv) with addition rate of 0.8 $\mu\text{L min}^{-1}$, NHPI (8 mg, 0.05 mmol, 0.1 equiv), molecular sieves (200 mg), 80 °C, 22 h. No NHPI was used for isolating the imides. ^bConversions and selectivities were determined by GC-MS based on concentration of amide and selectivity toward the imide product. ^cUsed Cs/Mn₂O₃ instead of AMO. All runs were repeated at least twice, with a standard deviation of below 10%. Isolated Yields are in Parentheses.

DFT calculation performed at MO6-2X for this reaction in the gas phase, this N-H hydrogen atom abstraction will have a 12 kcal/mol higher activation energy (E_a) barrier than α C-H atom abstraction. The reduction of Mn centers simultaneously generates the formation of labile lattice oxygen, which reoxidizes the Mn center with production of H₂O₂, which can easily be decomposed over manganese oxide and form water¹. Once formed, the α hydroperoxide intermediate can readily undergo a further abstraction of the 2nd benzylic hydrogen to yield the corresponding imide product. Hydroperoxide adducts were not detected by GC-MS, which signifies the rapid oxidation of the hydroperoxide species.

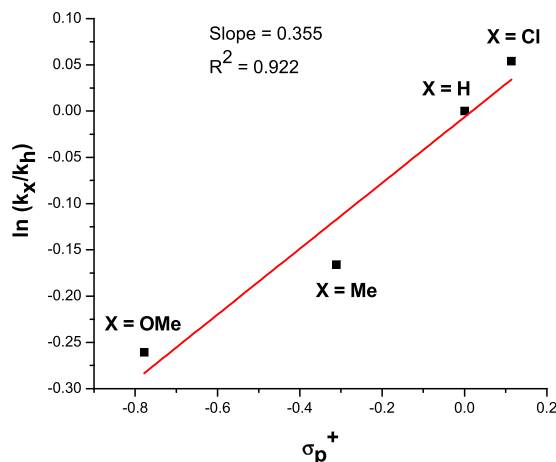


Figure 1. Hammett plot of competitive oxidation of para substituted *N*-benzylbenzamide. Reaction conditions are as described in Table 3 for 8 h. A linear relationship between $\ln(k_x/k_H)$ and Brown–Okamoto constant (σ_p^+) for para substituted benzylamines with slope (ρ) of 0.355 was obtained, which indicates the formation of a negatively charged transition state.

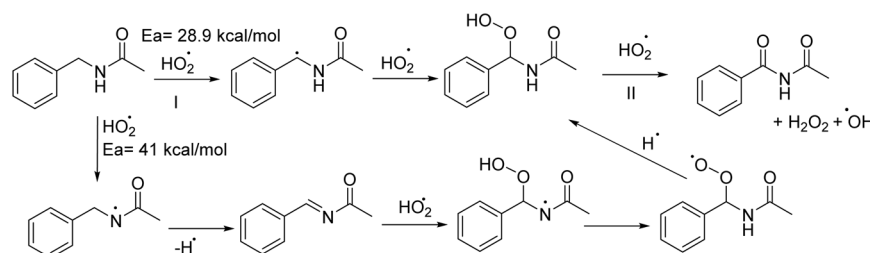


Figure 2. The C-H abstractions vs N-H abstraction pathways.

The aerobic oxidation pathway proceeds with meso Cs/Mn₂O₃ and AMO in the presence of NHPI. Perhaps a heterogeneous metal bound surface superoxide is formed as a first step^{41–43}. This would then subsequently converted to a bound hydroperoxide followed by a similar mechanism TBHP as described in Fig. 2. This mechanism resembles the formylamide oxidation with peroxide and NHPI with a Co(II) catalyst. The exact mechanism is still under investigation with an emphasis on identification of all reactive oxygen species and potential correlation to reaction rates.

One of the major obstacles observed for many heterogeneous catalyst systems is of the product not desorbing from the catalyst surface. We wanted to study if there was a possibility that this phenomenon was occurring for the *N*-benzylbenzamide oxidation reaction; so, additional pre- and post-reaction characterizations were performed. X-ray Fluorescence spectroscopy (Table S3) was also done in order to further quantify the amount of product adsorbed utilizing the most optimized conditions (Entry 1, Table 3). We were able to determine that there was approximately 5% by mass of the product still adsorbed on the catalyst. These additional characterizations allowed us to partially account for the gaps between GC-MS and isolated yields.

Conclusion

In summary, manganese oxide materials can catalyze the oxidation of aromatic substituted amides to imides. Among the several materials studied, mesoporous Cs promoted manganese oxide (meso Cs/Mn₂O₃) and amorphous manganese oxide (AMO) were shown to be the best catalysts. AMO oxidized a diverse array of aromatic amide derivatives to produce imides with high conversions and selectivities (90–100%). Although aerobic oxidation with meso Cs/Mn₂O₃ mediated by NHPI gave modest yields of imide, in the optimal procedure TBHP was used as oxidant. This manganese oxide mediated selective partial oxidation method is useful as compared to precious metal catalyst (e.g., Pt, Rh, Pd or Ir) that are used for partial oxidation in terms of activity, cost, and environmental impact.

Methods

Synthesis of manganese oxide materials. The manganese oxide materials were synthesized by well-established methods meso Cs/Mn₂O₃¹⁷, meso Mn₂O₃¹⁷, OMS-2 (SF)⁴⁴ and AMO⁴⁵.

Synthesis of meso Cs/Mn₂O₃. Manganese (II) nitrate tetrahydrate (0.02 mol) was dissolved in a 1-butanol solution containing 0.188 mol (14 g) 1-butanol, 0.032 mol (2 g) of HNO₃ and 3.4 × 10⁻⁴ mol (2 g) of P₁₂₃ surfactant in a 150 mL beaker at RT and under magnetic stirring¹⁷. To this clear aqueous solution, 100 mL of 2.0 M CsNO₃

was added maintaining the Mn:X ratio as 100:1. The resulting clear solution was then kept in an oven at 120 °C for 3 h under air. The resulting black powder was washed with excess ethanol, centrifuged and dried in vacuum oven overnight. The dried black powder was then heated to 150 °C for 12 h and 250 °C for 3 h under air. The powder diffraction pattern of the material at this calcination temperature appears amorphous. However, upon heating at 450 °C or higher the XRD peak of this materials starts to appear crystalline with a pattern of Mn₂O₃ (Bixbyite)¹⁷. Meso Mn₂O₃ was prepared using the same procedure without having the Cs ions.

Synthesis of OMS-2(SF). In a typical experiment, 9.48 g (0.06 mol) of KMnO₄ and 22.05 g (0.09 mol) of Mn(Ac)₂·4H₂O powders were mixed and ground homogeneously in a mortar⁴⁴. The mixed powders were then placed in an autoclave and heated at 80 °C for 4 h. The resulting black product was thoroughly washed with excess deionized water, and finally dried at 80 °C in air overnight.

Synthesis of AMO. A 60 mL volume of a 1.6 M Potassium permanganate solution was added dropwise to 100 mL of a 0.25 M Oxalic acid solution⁴⁵. The mixture was stirred at room temperature for 2 hours. The resulting mixture was filtered and then washed with excess deionized water. The sample was then dried overnight at 90 °C.

General procedure for oxidation of amides to imides. In a typical amide oxidation reaction, a mixture of *N*-benzylbenzamide (0.5 mmol, 100 mg), catalyst (50 mg), *N*-hydroxyphthalimide (10 mol%), molecular sieves (4A) and acetonitrile (5 mL) was added in a 50 mL two necked round bottom flask equipped with a condenser. A solution of tert-butylhydroperoxide (TBHP, 10 equiv) in nonane (5.5 M) was added dropwise with a rate of 0.8 microliter min⁻¹. The reaction mixture was heated to reflux under vigorous stirring (700 rpm) until the full consumption of TBHP. After reaction, the mixture was cooled and the catalyst was removed by filtration. The product analysis was done using GC-MS (gas chromatography-mass spectrometry). The conversion was determined based on the concentration of amides. Most reactions were repeated twice, and the average values were used. The imide products were isolated by silica gel column chromatography using hexane and (30–50%) ethyl acetate as the eluent and identified by ¹H and ¹³C NMR spectra.

Characterization. The GC-MS analyses were performed with a 7820A GC system connected with a mass detector of 5975 series MSD from Agilent Technologies and a nonpolar cross-linked methyl siloxane column with dimensions of 12 in × 0.200 mm × 0.33 μm was used. The ¹H and ¹³C NMR spectra were recorded on a Bruker AVANCE III- 400 MHz spectrometer. ¹H NMR spectra were collected at 400 MHz with chemical shift referenced to the residual CHCl₃ peak in CDCl₃ (δ: H 7.26 ppm). ¹³C NMR spectra were collected at 100 MHz and referenced to the CDCl₃ signal (δ: C 77.0 ppm)⁴⁶. Only in case of phthalimide the solvent was DMSO-d₆, and chemical shifts were referenced to the residual DMSO-d₅ peak in DMSO-d₆ (δ: H 2.50 ppm) for ¹H NMR and the DMSO-d₆ peak (δ: C 39.51 ppm) for ¹³C NMR⁴⁶. The spectral data of imide products were compared with the literature reports⁴⁷.

References

- Vanderwal, C. D. & Jacobsen, E. N. Enantioselective Formal Hydration of α,β-Unsaturated Imides by Al-Catalyzed Conjugate Addition of Oxime Nucleophiles. *J. Am. Chem. Soc.* **126**, 14724–14725 (2004).
- Balskus, E. P. & Jacobsen, E. N. α,β-Unsaturated β-Silyl Imide Substrates for Catalytic, Enantioselective Conjugate Additions: A Total Synthesis of (+)-Lactacystin and the Discovery of a New Proteasome Inhibitor. *J. Am. Chem. Soc.* **128**, 6810–6812 (2006).
- Ali, M. A., Siddiki, S. M. A. H., Kon, K., Hasegawa, J. & Shimizu, K. Versatile and Sustainable Synthesis of Cyclic Imides from Dicarboxylic Acids and Amines by Nb₂O₅ as a Base-Tolerant Heterogeneous Lewis Acid Catalyst. *Chem. – A Eur. J.* **20**, 14256–14260 (2014).
- Nicolaou, K. C. & Mathison, C. J. N. Synthesis of Imides, *N*-Acyl Vinyllogous Carbamates and Ureas, and Nitriles by Oxidation of Amides and Amines with Dess–Martin Periodinane. *Angew. Chemie Int. Ed.* **44**, 5992–5997 (2005).
- De Sarkar, S. & Ackermann, L. Ruthenium(II)-Catalyzed C–H Activation with Isocyanates: A Versatile Route to Phthalimides. *Chem. – A Eur. J.* **20**, 13932–13936 (2014).
- Minisci, F., Punta, C., Recupero, F., Fontana, F. & Pedulli, G. F. Aerobic Oxidation of *N*-Alkylamides Catalyzed by *N*-Hydroxyphthalimide under Mild Conditions. Polar and Enthalpic Effects. *J. Org. Chem.* **67**, 2671–2676 (2002).
- Bietti, M. *et al.* Kinetic Study of the Reaction of the Phthalimide-*N*-oxyl Radical with Amides: Structural and Medium Effects on the Hydrogen Atom Transfer Reactivity and Selectivity. *J. Org. Chem.* **81**, 11924–11931 (2016).
- Taherpour, A. A., Abramian, A. & Kardanyazd, H. Synthesis of Imide by Oxidation of *N*-Alkyl Amides under Microwave Irradiation. *Chinese J. Org. Chem.* **27**, 123–125 (2007).
- Gupta, R. B. *Hydrogen Fuel: Production, Transport, and Storage*. (CRC Press, 2009).
- Brock, S. L. *et al.* A Review of Porous Manganese Oxide Materials. *Chem. Mater.* **10**, 2619–2628 (1998).
- Suib, S. L. Porous Manganese Oxide Octahedral Molecular Sieves and Octahedral Layered Materials. *Acc. Chem. Res.* **41**, 479–487 (2008).
- Tian, Z.-R. *et al.* Manganese Oxide Mesoporous Structures: Mixed-Valent Semiconducting Catalysts. *Science (80-)*. **276**, 926 LP-930 (1997).
- Post, J. E. Manganese oxide minerals: Crystal structures and economic and environmental significance. *Proc. Natl. Acad. Sci.* **96**, 3447–3454 (1999).
- Kim, S. C. & Shim, W. G. Catalytic combustion of VOCs over a series of manganese oxide catalysts. *Appl. Catal. B Environ.* **98**, 180–185 (2010).
- Nicolas-Tolentino, E., Tian, Z.-R., Zhou, H., Xia, G. & Suib, S. L. Effects of Cu²⁺ Ions on the Structure and Reactivity of Todorokite- and Cryptomelane-Type Manganese Oxide Octahedral Molecular Sieves. *Chem. Mater.* **11**, 1733–1741 (1999).
- Poyraz, A. S. *et al.* Bimodification of Mesoporous Silicon Oxide by Coupled 'In Situ Oxidation at the Interface and Ion Exchange' and its Catalytic Activity in the Gas-Phase Toluene Oxidation. *ChemCatChem* **5**, 920–930 (2013).
- Biswas, S. *et al.* Ion induced promotion of activity enhancement of mesoporous manganese oxides for aerobic oxidation reactions. *Appl. Catal. B Environ.* **165**, 731–741 (2015).
- Santos, V. P., Pereira, M. F. R., Orfão, J. J. M. & Figueiredo, J. L. Catalytic oxidation of ethyl acetate over a cesium modified cryptomelane catalyst. *Appl. Catal. B Environ.* **88**, 550–556 (2009).

19. Son, Y.-C., Makwana, V. D., Howell, A. R. & Suib, S. L. Efficient, Catalytic, Aerobic Oxidation of Alcohols with Octahedral Molecular Sieves. *Angew. Chemie* **113**, 4410–4413 (2001).
20. Opembe, N. N., Son, Y.-C., Sriskandakumar, T. & Suib, S. L. Kinetics and Mechanism of 9H-Fluorene Oxidation Catalyzed by Manganese Oxide Octahedral Molecular Sieves. *ChemSusChem* **1**, 182–185 (2008).
21. Ghosh†, R. *et al.* Role of Manganese Oxide Octahedral Molecular Sieves in Styrene Epoxidation, <https://doi.org/10.1021/JP056961N> (2006).
22. Wang, Y., Kobayashi, H., Yamaguchi, K. & Mizuno, N. Manganese oxide-catalyzed transformation of primary amines to primary amides through the sequence of oxidative dehydrogenation and successive hydration. *Chem. Commun.* **48**, 2642 (2012).
23. Yamaguchi, K., Kobayashi, H., Oishi, T. & Mizuno, N. Heterogeneously Catalyzed Synthesis of Primary Amides Directly from Primary Alcohols and Aqueous Ammonia. *Angew. Chemie Int. Ed.* **51**, 544–547 (2012).
24. Yamaguchi, K. *et al.* Green oxidative synthesis of primary amides from primary alcohols or aldehydes catalyzed by a cryptomelane-type manganese oxide-based octahedral molecular sieve, OMS-2. *318 Catal. Sci. Technol. Catal. Sci. Technol.* **3**, 318–327 (2013).
25. Wang, Y., Yamaguchi, K. & Mizuno, N. Manganese Oxide Promoted Liquid-Phase Aerobic Oxidative Amidation of Methylarenes to Monoamides Using Ammonia Surrogates. *Angew. Chemie* **124**, 7362–7365 (2012).
26. Yamaguchi, K., Wang, Y. & Mizuno, N. Manganese Oxide-catalyzed Additive- and Solvent-free Aerobic Oxidative Synthesis of Primary Amides from Primary Amines. *Chem. Lett.* **41**, 633–635 (2012).
27. Sithambaram, S., Kumar, R., Son, Y. & Suib, S. Tandem catalysis: Direct catalytic synthesis of imines from alcohols using manganese octahedral molecular sieves. *J. Catal.* **253**, 269–277 (2008).
28. Chen, B. *et al.* Direct imine formation by oxidative coupling of alcohols and amines using supported manganese oxides under an air atmosphere. *Green Chem.* **16**, 3328 (2014).
29. Zhang, Z. *et al.* tert-Butyl hydroperoxide (TBHP)-mediated oxidative self-coupling of amines to imines over a α -MnO₂ catalyst. <https://doi.org/10.1039/c3gc42312c>.
30. Jin, X. *et al.* Heterogeneously catalyzed selective aerobic oxidative cross-coupling of terminal alkynes and amides with simple copper(ii) hydroxide. *Chem. Commun.* **48**, 4974 (2012).
31. Yamaguchi, K., Wang, Y., Oishi, T., Kuroda, Y. & Mizuno, N. Heterogeneously Catalyzed Aerobic Cross-Dehydrogenative Coupling of Terminal Alkynes and Monohydrosilanes by Gold Supported on OMS-2. *Angew. Chemie Int. Ed.* **52**, 5627–5630 (2013).
32. Jin, X., Yamaguchi, K. & Mizuno, N. Aerobic cross-dehydrogenative coupling of terminal alkynes and tertiary amines by a combined catalyst of Zn²⁺ and OMS-2. <https://doi.org/10.1039/c4ra05105j>.
33. Yu, H., Chen, Y. & Zhang, Y. TBHP/TEMPO-Mediated Oxidative Synthesis of Imides from Amides. *Chinese J. Chem.* **33**, 531–534 (2015).
34. Poyraz, A. S., Kuo, C.-H., Biswas, S., King'ondo, C. K. & Suib, S. L. A general approach to crystalline and monomodal pore size mesoporous materials. *Nat. Commun.* **4**, 2952 (2013).
35. Biswas, S. *et al.* Aerobic Oxidation of Amines to Imines by Cesium-Promoted Mesoporous Manganese Oxide. *ACS Catal.* **5**, 4394–4403 (2015).
36. Dutta, B. *et al.* Mesoporous Manganese Oxide Catalyzed Aerobic Oxidative Coupling of Anilines To Aromatic Azo Compounds. *Angew. Chemie Int. Ed.* **55**, 2171–2175 (2016).
37. Tang, R.-Y. *et al.* TBHP-mediated oxidative thiolation of an sp³ C–H bond adjacent to a nitrogen atom in an amide. *Chem. Commun.* **47**, 12867 (2011).
38. Grootboom, N. & Nyokong, T. Iron perchlorophthalocyanine and tetrasulfophthalocyanine catalyzed oxidation of cyclohexane using hydrogen peroxide, chloroperoxybenzoic acid and tert-butylhydroperoxide as oxidants. *J. Mol. Catal. A Chem.* **179**, 113–123 (2002).
39. Sheldon, R. A. & Arends, I. W. C. E. Organocatalytic Oxidations Mediated by Nitroxyl Radicals. *Adv. Synth. Catal.* **346**, 1051–1071 (2004).
40. Hermans, I. *et al.* Mechanism of the catalytic oxidation of hydrocarbons by N-hydroxyphthalimide: a theoretical study. Electronic supplementary information (ESI) available: all discussed TS and important intermediates (geometries, energies, ZPE, rotational constants and frequencies). *Chem. Commun.* **05**, 1140, <http://www.rsc.org/suppdata/cc/b4/b401050g/> (2004).
41. Ishii, Y., Iwahama, T., Sakaguchi, S., Nakayama, K. & Nishiyama, Y. Alkane Oxidation with Molecular Oxygen Using a New Efficient Catalytic System: N-Hydroxyphthalimide (NHPI) Combined with Co(acac)(n) (n = 2 or 3). *J. Org. Chem.* **61**, 4520–4526 (1996).
42. Ishii, Y. & Sakaguchi, S. Recent progress in aerobic oxidation of hydrocarbons by N-hydroxyimides. *Catal. Today* **117**, 105–113 (2006).
43. Shibamoto, A., Sakaguchi, S. & Ishii, Y. Aerobic Oxidation of Methylpyridines to Pyridinecarboxylic Acids Catalyzed by N-Hydroxyphthalimide. *Org. Process Res. Dev.* **4**, 505–508 (2000).
44. Ding, Y. S. *et al.* Synthesis and catalytic activity of cryptomelane-type manganese dioxide nanomaterials produced by a novel solvent-free method. *Chem. Mater.* **17**, 5382–5389 (2005).
45. Cao, H. & Suib, S. L. Highly efficient heterogeneous photooxidation of 2-propanol to acetone with amorphous manganese oxide catalysts. *J. Am. Chem. Soc.* **116**, 5334–5342 (1994).
46. Gottlieb, H. E., Kotlyar, V. & Nudelman, A. NMR chemical shifts of common laboratory solvents as trace impurities. *J. Org. Chem.* **62**, 7512–7515 (1997).
47. Evans, D. A., Nagorny, P. & Xu, R. Ceric ammonium nitrate promoted oxidation of oxazoles. *Org. Lett.* **8**, 5669–5671 (2006).

Acknowledgements

This work was funded by ExxonMobil Research and Engineering Company. We acknowledge the US Department of Energy, Office of Basic Energy Sciences, Division of Chemical, Biological and Geological Sciences under grant DE-FG02-86ER13622.A000 for partial support of this research. S.B. thanks Anton Gudz and Dr. Lakshitha Pahalagedara for helping in synthesis.

Author Contributions

S.B., P.N. and S.L.S. designed the experiments. S.B. synthesized the materials and conducted the catalytic reactions. H.K. and Q.A.N. performed some initial optimization studies. D.R.C. and K.T.C. isolated the imide products. A.R.H. provided valuable insight. S.R. performed computational studies. S.L.S. and P.N. were the project coordinators. S.B., P.N. and S.L.S. prepared the manuscript. All authors have read and approved the final manuscript.

Additional Information

Supplementary information accompanies this paper at <https://doi.org/10.1038/s41598-018-31729-3>.

Competing Interests: The authors declare no competing interests.

Publisher's note: Springer Nature remains neutral with regard to jurisdictional claims in published maps and institutional affiliations.



Open Access This article is licensed under a Creative Commons Attribution 4.0 International License, which permits use, sharing, adaptation, distribution and reproduction in any medium or format, as long as you give appropriate credit to the original author(s) and the source, provide a link to the Creative Commons license, and indicate if changes were made. The images or other third party material in this article are included in the article's Creative Commons license, unless indicated otherwise in a credit line to the material. If material is not included in the article's Creative Commons license and your intended use is not permitted by statutory regulation or exceeds the permitted use, you will need to obtain permission directly from the copyright holder. To view a copy of this license, visit <http://creativecommons.org/licenses/by/4.0/>.

© The Author(s) 2018